

## USE OF COUPLED FINITE ELEMENT ANALYSIS IN UNSATURATED SOIL PROBLEMS

A. K. L. NG<sup>1\*</sup> AND J. C. SMALL<sup>2</sup>

<sup>1</sup> *Binnie Black & Veatch Hong Kong Limited, 11/F New Town Tower, Shatin, N.T., Hong Kong*

<sup>2</sup> *Department of Civil Engineering, The University of Sydney, NSW 2006, Australia*

### SUMMARY

This paper presents a variation of Biot's consolidation theory for analysing problems involving unsaturated soils, and implemented using the finite element method. The numerical method is applied to a few geotechnical problems as examples and the results obtained are compared to some published data. The illustrative examples show how the numerical method can be used to analyse seepage and consolidation problems associated with unsaturated soils and demonstrate the flexibility and applicability of the presented method. Copyright © 2000 John Wiley & Sons, Ltd.

KEY WORDS: Biot's consolidation theory; unsaturated soils; finite element method

### INTRODUCTION

Many classic soil mechanics theories were developed for saturated soils which comprise soil grains and pore water. In reality, unsaturated soils are often encountered. Compacted fills are good examples where the soils are unsaturated and contain pore air. The subject of unsaturated soils has been receiving attention increasingly for the last few decades. Some researchers have developed new concepts and theories to investigate and capture the observed behaviour of unsaturated soils.<sup>1–8</sup> Some researchers on the other hand focused on analysing geotechnical problems such as seepage and consolidation problems, involving unsaturated soils.<sup>9–14</sup> Coupled formulations that involve the air and water phases in soils have also been presented.<sup>15–17</sup> However, because of the great complexity of the three-phase models, extensive and specially designed soil testing is required to determine the properties of the soil–air–water mixture, and this can prove to be expensive in current practice.

In this paper, a simplified coupled formulation also based on Biot's theory<sup>18</sup> for solving geotechnical problems associated with unsaturated soils is presented, and a numerical solution of the proposed formulation has been developed using the finite element technique. The formulation has been developed by noting that the air and water pressures in unsaturated soils are approximately equal at high degrees of saturation. This led to a relatively simple formulation which can have a range of practical applications.

\* Correspondence to: A. K. L. Ng, Binnie Black & Veatch Hong Kong Ltd., 11/F New Town Tower, Pak Hok Ting St., Shatin, N.T., Hong Kong. Tel: (852) 26011000 Fax: (852) 26013988 E-mail: axelng@netvigator.com

Since the equilibrium and continuity field equations are coupled in Biot's theory, analyses based on the theory are often referred to as coupled analyses. In the research area of unsaturated soils, attempts had been made in the past by some researchers to modify Biot's consolidation theory which was initially developed for saturated soils, for solving unsaturated soil problems. Some of the researchers postulated the pore water and pore air as a homogeneous and compressible fluid.<sup>9,11</sup> The compressibility of the 'homogeneous' fluid was expressed as functions of different parameters, such as pore water pressure and degree of saturation. In terms of continuity, the volume of water leaving or entering a soil element of a finite size, would depend on the change in pore space as well as the amount that the fluid was compressed. Another group of researchers considered the continuity from the view point of changes in storage of moisture or the volumetric moisture content in unsaturated soils,<sup>10,13</sup> and the storage of moisture of the soils was assumed to be governed by pore water pressure.

In this paper, it will be shown that while the above two approaches for modifying Biot's theory are rather different in concept, they can be considered within a single mathematical framework. A numerical method based on the framework is derived using the finite element technique. The numerical method is then applied to a range of geotechnical problems as an illustration.

The problems analysed include modelling of generation of pore water pressure in unsaturated soils under isotropic compression in triaxial tests, a classical strip footing problem and a seepage problem involving rapid drawdown. These problems were chosen to demonstrate the flexibility and applicability of the numerical method when applied to problems which otherwise might have to be analysed with different and specialized methods. The results of the presented analyses have also been compared to published data in the literature.

The results of the analyses have been encouraging. And it has been demonstrated that the modified Biot's theory can be used to provide a simple framework for analysing a range of geotechnical problems involving unsaturated soils.

## THEORY

### *Biot's consolidation theory*

Biot's equations governing the consolidation of a saturated porous medium may be written in a general form

$$\frac{\partial \sigma_{ij}}{\partial x_j} - F_i = 0 \quad (1a)$$

$$\sigma'_{ij} = \sigma_{ij} - q\delta_{ij} = -H_{ijkl}\varepsilon_{kl} \quad (1b)$$

$$\varepsilon_{kl} = \frac{1}{2}(u_{k,l} + u_{l,k}) \quad (1c)$$

$$\frac{\partial v_i}{\partial x_i} = \frac{\partial \theta}{\partial t} \quad (1d)$$

$$v_i = -\frac{k}{\gamma_w} \frac{\partial q}{\partial x_j} \quad (1e)$$

where  $i$  and  $j$  denote directions in a Cartesian reference system,  $\sigma_{ij}$  and  $\sigma'_{ij}$  are components of total and effective stresses,  $F_i$  are components of body force,  $q$  is the pore water pressure,  $\delta_{ij}$  is the Kronecker delta,  $H_{ijkl}$  are the coefficients relating stress increments to strain increments for some constitutive law,  $\varepsilon_{kl}$  are the components of the strain tensor,  $u_i$  are the components of displacement,  $v_i$  are the components of the superficial velocity,  $\theta$  is the volumetric strain ( $\theta = \varepsilon_{ii}$ ),  $t$  is time,  $k_{ij}$  are the Darcy's coefficients of permeability, and  $\gamma_w$  is the unit weight of water.

The governing equations can be solved using a finite element approximation.<sup>19</sup> The resulting finite element equations can be expressed in an incremental form;<sup>20</sup>

$$\begin{bmatrix} \mathbf{K} & -\gamma_w \mathbf{L}^T \\ -\gamma_w \mathbf{L} & -\alpha \Delta t \gamma_w \Phi \end{bmatrix} \begin{Bmatrix} \Delta \mathbf{\delta} \\ \Delta \mathbf{h} \end{Bmatrix} = \begin{Bmatrix} \Delta \mathbf{g} \\ \Delta t \gamma_w \Phi \mathbf{h}_t \end{Bmatrix} \quad (2)$$

where  $\mathbf{\delta}$  and  $\mathbf{h}$  are vectors containing the nodal displacements and total water heads, respectively.

$\mathbf{K}$  is the stiffness matrix,

$$\mathbf{K} = \int_V \mathbf{B}^T \mathbf{D} \mathbf{B} dV \quad (3)$$

$\Phi$  is the flow matrix,

$$\Phi = \int_V \mathbf{E}^T \mathbf{k} \mathbf{E} dV \quad (4)$$

$\mathbf{L}$  is the coupling matrix,

$$\mathbf{L} = \int_V \mathbf{a} \mathbf{d}^T dV \quad (5)$$

and  $\Delta \mathbf{g}$  is the out of balance force vector,

$$\Delta \mathbf{g} = \int_V \mathbf{B}^T \boldsymbol{\sigma}'_t dV + \gamma_w \mathbf{L}^T (\mathbf{h}_t - \mathbf{h}_{cl}) + \int_V \mathbf{N}^T \mathbf{F}_{t+\Delta t} dV + \int_S \mathbf{N}^T \mathbf{T}_{t+\Delta t} dS \quad (6)$$

The following are the definitions of the terms in equations (3)–(6),

$\mathbf{B}$  is the displacement–strain matrix,

$\mathbf{D}$  is the stress–strain matrix,

$\mathbf{E}$  contains the derivatives of the shape functions,

$\mathbf{k}$  is the matrix of permeability coefficients,

$\mathbf{a}$  is the vector of shape functions,

$\mathbf{d}$  is the vector relating nodal displacement to volumetric strain,

$\boldsymbol{\sigma}'$  is the effective stress vector,

$\mathbf{N}$  contains the shape functions,

$\mathbf{F}$  is the body force vector,

$\mathbf{T}$  is the traction vector.

The first three terms in the expression for  $\Delta \mathbf{g}$  allow forces created by excavation or construction to be considered. If only surface tractions exist, only the last term is necessary.

When the soil skeleton is assumed to deform in a non-linear manner or the permeability of the soil is changing, the equations for the coupled deformation are similar, but the stiffness matrix

and the flow matrix need to be set up at each time step as they are not constant. This has been discussed by Siriwardane and Desai,<sup>21</sup> who present numerical solutions for non-linear soil consolidation problems.

#### *Governing equations for unsaturated soils*

In this paper, the constitutive relationship for unsaturated soils is assumed to be governed by two stress variables; effective stress in the soil skeleton and pore water pressure, as in some previous work in the literature.<sup>9,11</sup> In reality, the pore air pressure and water pressure are not the same in an unsaturated soil. However, at higher degrees of saturation, the pore air pressure and pore water pressure are approximately equal,<sup>22</sup> especially when the changes of pore water pressures are positive. The pore water pressures and pore air pressures are generally fairly close to each other for degrees of saturation above about 80 per cent. This degree of saturation depends on the type of soil, and would need to be established for a particular soil type. Thus the effective stress law (equation (1b)) may be assumed to apply for unsaturated soils at or above such degree of saturation, as pressures in the pore fluids are approximately equal. In this paper, the unsaturated soils are assumed to be either elastic or behave as Modified Cam-clay materials.

Now, the continuity equation for unsaturated soils is considered. To develop the equation, we consider an infinitesimal element of an unsaturated soil with sides being parallel with the Cartesian co-ordinate axes  $x$ ,  $y$  and  $z$ . The continuity equation of the element in terms of water flow can be written by considering the rate of change of the volumetric moisture content,

$$\nabla^T v = \frac{\partial \theta_m}{\partial t} \quad (7)$$

where  $v$  is the vector of superficial velocities of water.  $\nabla$  is an operator vector for directions  $x$ ,  $y$  and  $z$ .  $\theta_m$  is the volumetric moisture content and by definition,

$$\theta_m = \frac{V_w}{V} = n S_r \quad (8)$$

where  $V_w$  and  $V$  are the volume of pore water and total volume of the soil element, respectively,  $n$  is porosity and  $S_r$  is degree of saturation of the soil.

Combining equations (7) and (8), and expanding leads to

$$\nabla^T v = n \frac{\partial S_r}{\partial t} + S_r \frac{\partial n}{\partial t} \quad (9)$$

If the soil grains are incompressible and infinitesimal strain is considered, the rate of change of porosity is equal to the rate of change of volumetric strain,

$$\frac{\partial n}{\partial t} = \frac{\partial \theta}{\partial t} \quad (10)$$

Substituting equation (10) into (9) and rearranging gives

$$\nabla^T v - S_r \frac{\partial \theta}{\partial t} = n \frac{\partial S_r}{\partial t} \quad (11)$$

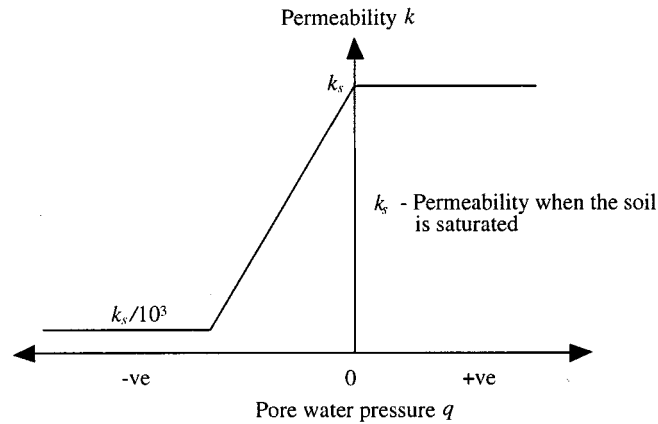


Figure 1. Idealization of the permeability – pore water pressure relationship

It should be noted that when the degree of saturation is equal to unity and remains constant (i.e.  $S_r = 1$  and  $\partial S_r / \partial t = 0$ ), the continuity equation (11) is reduced to that for the saturated medium:

$$\nabla^T v - \frac{\partial \theta}{\partial t} = 0 \quad (12)$$

The determination and physical meanings of some of the terms in equation (11) warrant some detailed discussions.

The superficial velocity of water flow in unsaturated soils, presented by  $v$  in equation (11) is commonly described using Darcy's law. However, the permeability in unsaturated soils was found to decrease when the pore water pressure is negative. Bouwer<sup>23</sup> provided a collection of the relationships between permeability and negative pore water pressure for different types of soils.

Various simplified forms of the permeability–pore water pressure relationship were employed in some previous finite element analyses for seepage problems.<sup>24–27</sup> An idealized relationship as shown in Figure 1 is adopted for the present numerical method.

To evaluate the right-hand side of equation (11), the concept adopted by Neuman<sup>28</sup> is employed in which the volumetric moisture content is assumed to depend on pore water pressure only,

$$C(q) = \frac{\partial \theta_m}{\partial q} = \frac{\partial (n S_r)}{\partial q} \quad (13)$$

where  $q$  is the pore water pressure and  $C$  is the specific moisture capacity which is governed by pore water pressure. The relationship between volumetric moisture content and negative pore water pressure can be determined experimentally. Figure 2 shows the curves reported by Lam *et al.*<sup>12</sup>

Assuming the strain is small and hence the porosity  $n$  is almost constant, equation (13) can be written as

$$C(q) = n \frac{\partial S_r}{\partial q} \quad (14)$$

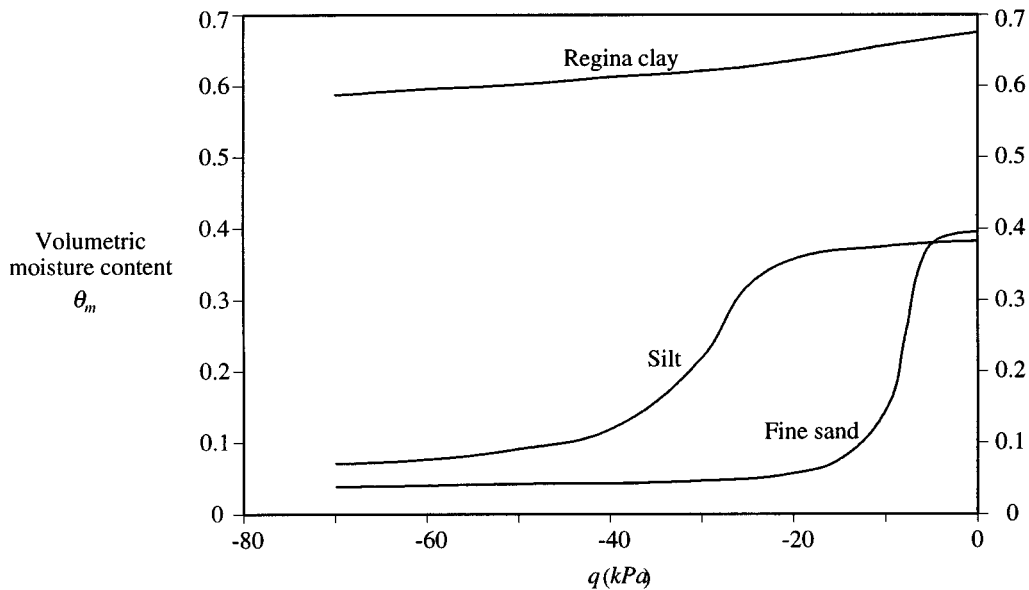


Figure 2. Variation of volumetric moisture content with negative pore water pressure<sup>12</sup>

The direct relationship between the degree of saturation and pore water pressure has also been investigated by Lloret and Alonso,<sup>29</sup> and a state surface for the degree of saturation  $S_r$  was established in  $\sigma - u_a$  and  $u_a - q$  space, where  $\sigma$  and  $u_a$  are the total stress and pore air pressure, respectively.

Relationships between degree of saturation and negative pore water pressure were adopted by Akai *et al.*<sup>10</sup> and Kohgo and Yamashita<sup>13</sup> in deriving their coupled formulations for unsaturated soils based on Biot's theory. However, the use of the relationship for a positive range of pore water pressures was not explored. Ghaboussi and Wilson,<sup>9</sup> and Chang and Duncan<sup>11</sup> used a different concept to describe the continuity equation when the pore pressure is positive. They assumed the pore water and air behaved as a single compressible fluid. Based on this assumption, a compressibility term was introduced to the continuity equation<sup>11</sup> instead of the rate of change of degree of saturation (or storage) term in equation (11).

Although the compressibility of the pore air fluid can be accounted for by using a compressibility term in the continuity equation, the characteristics of the pore air and water can also be described using a degree of saturation-pore water pressure relationship as for the negative range of pore water pressure. In fact, this relationship has been studied in the past in order to apply adequate back pressure to saturate triaxial test samples. By considering the compression and solution of the pore air in unsaturated soils, a theoretical relationship has been proposed by Lowe and Johnson,<sup>30</sup> and Mitchell *et al.*,<sup>31</sup>

$$S_r = \frac{0.0099q + 0.98S_{r0}}{0.98 + 0.0097q} \quad (15)$$

where  $S_r$  is the degree of saturation at a pore water pressure  $q$  in kPa.  $S_{r0}$  denotes the degree of saturation at zero pore water pressure. By using equation (15) for positive pore water pressure, the

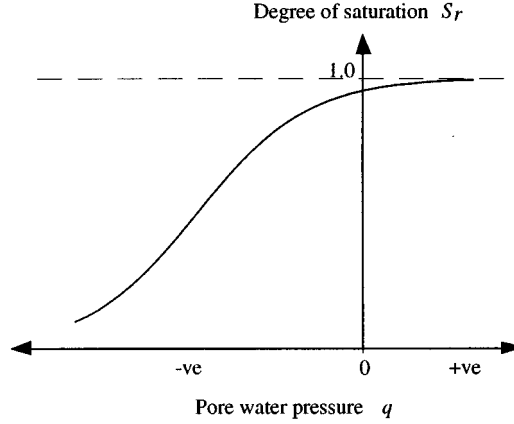


Figure 3. Relationship of degree of saturation and pore water pressure

variation of degree of saturation with pore water pressures in positive and negative ranges can be represented by a simple curve as shown in Figure 3.

Now  $S_r$  can be expressed as a function of pore water pressure  $q$  for the positive and negative ranges, and the right hand side of equation (11) can be expressed as

$$n \frac{\partial S_r}{\partial t} = n \frac{\partial S_r}{\partial q} \frac{\partial q}{\partial t} = \gamma_w \frac{\partial S_r}{\partial q} \frac{\partial h}{\partial t} \quad (16)$$

where  $h$  is total water head.

Now substituting equation (16) into (11), it follows that

$$\nabla^T v - S_r \frac{\partial \theta}{\partial t} = n \gamma_w \frac{\partial S_r}{\partial q} \frac{\partial h}{\partial t} \quad (17)$$

#### Finite element equations

The continuity equation (17) derived above can be solved using the virtual work principle within the finite element framework as for saturated porous media.<sup>32</sup> This finite element equation when coupled with the finite element equation for equilibrium, can be expressed as

$$\begin{bmatrix} \bar{\mathbf{K}} & -\gamma_w \mathbf{L}^T \\ -\gamma_w \mathbf{L} & -\alpha \Delta t \gamma_w \bar{\Phi}_{S_r} - \gamma_w \bar{\mathbf{Q}} \end{bmatrix} \begin{Bmatrix} \delta_{t+\Delta t} - \delta_t \\ \mathbf{h}_{t+\Delta t} - \mathbf{h}_t \end{Bmatrix} = \begin{Bmatrix} \Delta \mathbf{g} \\ \Delta t \gamma_w \bar{\Phi}_{S_r} \mathbf{h}_t \end{Bmatrix} \quad (18)$$

It can be shown that the set of equations (18) which has been developed for unsaturated soils, has an additional matrix when compared to the set of equations for a saturated soil (equation (2)). Matrix  $\mathbf{Q}$  represents the change of storage of moisture with respect to change in water head. For identification purposes,  $\mathbf{Q}$  is called the storage matrix here,

$$\mathbf{Q} = \int_V \frac{n \gamma_w}{S_r} \frac{\partial S_r}{\partial q} \mathbf{a} \mathbf{a}^T dV \quad (19)$$

and  $\bar{\Phi}_{S_r}$  is the flow matrix which is also a function of degree of saturation;

$$\Phi_{S_r} = \int_V \frac{1}{S_r} \mathbf{E}^T \mathbf{k} \mathbf{E} dV \quad (20)$$

Since matrices  $\mathbf{K}$ ,  $\Phi_{S_r}$  and  $\mathbf{Q}$  in equation (18) may change with the stresses or pore water pressures over the time step, the bar symbol is introduced to denote some average or representative values over the time step. In this paper, matrices  $\bar{\Phi}_{S_r}$  and  $\mathbf{Q}$  are evaluated for intermediate values of  $\mathbf{h}$ , e.g.,

$$\bar{\Phi}_{S_r} = \Phi_{S_r} \left( \frac{\mathbf{h}_t + \mathbf{h}_{t+\Delta t}}{2} \right) \quad (21)$$

and  $\mathbf{K}$  is evaluated for intermediate values of effective stresses.

To solve the non-linear equation (18), the Newton–Raphson method has been used. The method involves iteration and it is assumed that the solution can be written as

$$\delta_{t+\Delta t}^i = \delta_{t+\Delta t}^{i-1} + \Delta \delta_{t+\Delta t}^i \quad (22)$$

$$\mathbf{h}_{t+\Delta t}^i = \mathbf{h}_{t+\Delta t}^{i-1} + \Delta \mathbf{h}_{t+\Delta t}^i \quad (23)$$

where superscripts  $i$  and  $i-1$  denote the current and last iterations, respectively.

Substituting equations (22) and (23) into equation (18), a set of linear equations can be found,

$$\begin{bmatrix} \bar{\mathbf{K}}^{i-1} & -\gamma_w \mathbf{L}^T \\ -\gamma_w \mathbf{L} & -\alpha \Delta t \gamma_w \bar{\Phi}_{S_r}^{i-1} - \gamma_w \bar{\mathbf{Q}}^{i-1} \end{bmatrix} \begin{Bmatrix} \Delta \delta_{t+\Delta t}^i \\ \Delta \mathbf{h}_{t+\Delta t}^i \end{Bmatrix} = \begin{Bmatrix} \Delta \mathbf{g} - \bar{\mathbf{K}}^{i-1} (\delta_{t+\Delta t}^{i-1} - \delta_t) + \gamma_w \mathbf{L}^T (\mathbf{h}_{t+\Delta t}^{i-1} - \mathbf{h}_t) \\ (1 - \alpha) \Delta t \gamma_w \bar{\Phi}_{S_r}^{i-1} \mathbf{h}_t + \alpha \Delta t \gamma_w \bar{\Phi}_{S_r}^{i-1} \mathbf{h}_{t+\Delta t}^{i-1} \\ + \gamma_w \mathbf{L} (\delta_{t+\Delta t}^{i-1} - \delta_t) + \gamma_w \bar{\mathbf{Q}}^{i-1} (\mathbf{h}_{t+\Delta t}^{i-1} - \mathbf{h}_t) \end{Bmatrix} \quad (24)$$

where the values of the matrices are also allowed to change during iteration, for example,

$$\bar{\Phi}_{S_r}^{i-1} = \Phi_{S_r} \left( \frac{\mathbf{h}_t - \mathbf{h}_{t+\Delta t}^{i-1}}{2} \right) \quad (25)$$

When rigid media are considered, the continuity equation in equation (24) is in effect similar to that of the “residual flow procedure” developed by Desai and coworkers<sup>33–34</sup> in which the amount of water released by the soil when the water table is falling is applied to a finite element mesh as a flow across the free surface and the flow is treated mathematically as a correction term in the solution.

For every time step, equation (24) is solved repeatedly in an iteration loop until the increments in the solution  $\Delta \delta_{t+\Delta t}^i$  and  $\Delta \mathbf{h}_{t+\Delta t}^i$  are negligible. The convergence criterion used is that the maximum change of the increments ( $\Delta \delta_{t+\Delta t}^i$  and  $\Delta \mathbf{h}_{t+\Delta t}^i$ ) must be less than 1000th of the maximum term of the accumulated increment ( $\delta_{t+\Delta t}^i - \delta_t$  and  $\mathbf{h}_{t+\Delta t}^{i-1} - \mathbf{h}_t$ ). The solution obtained can then be used to create new initial conditions for the following time step. Thus the solution process can be repeated and marched forward in time.



## EXAMPLES

A FORTRAN computer program based on the coupled formulation (equation (24)) above was developed at the Centre for Geotechnical Research of the University of Sydney. The program has been used to analyse the following geotechnical problems as examples and to gain greater understanding of the problems.

### *Isotropic compression of unsaturated soils*

The first example is an illustration of how the numerical method can be used to estimate generation of pore water pressure in unsaturated soil under compression. In this case, the unsaturated soil is expected to increase in degree of saturation as pore water pressure develops.

The generation of pore water pressure in unsaturated soils under compression or shearing is related to many types of geotechnical problems and has been a subject receiving much attention. Early works by Skempton<sup>1</sup> are widely accepted as the method to estimate pore water pressure generated due to isotropic compression or application of deviator stress. In his work, coefficients  $A$  and  $B$  were proposed to estimate pore water pressure due to deviator stress and isotropic compression respectively. Coefficients  $A$  and  $B$  can be determined experimentally. Coefficient  $B$  is a function of relative compressibility of the pore fluids (air and water) and soil skeleton. The numerical method presented here has a fundamental difference from Skempton's work. Coefficients  $A$  and  $B$  are soil coefficients which combine the volume change characteristics of the soil skeleton and pore fluids. The present method on the other hand separates the compressibilities of the fluid and soil skeleton. The behaviour of the soil skeleton is assumed to be governed by the chosen constitutive relationships and the effective stresses, and the compressibility of the pore fluids is governed by the degree of saturation-pore water relationship.

The proposed numerical method is applied to model the generation of pore water pressure of a compacted fill under isotropic compression. The characteristic of the compacted fill was reported by Penman.<sup>35</sup> The compacted fill was used in constructing a major embankment dam in Britain at the time on the river Daer, designed by Binnie, Deacon and Gourley. The material was a boulder clay fill. Stability analyses carried out at the time indicated that the pore water pressure in the fill had to be less than 40 per cent of the overburden pressure to give a satisfactory factor of safety. Thus the generation of pore water pressure during construction was a great concern. Penman studied the compressibility of the fills compacted to different moisture contents using oedometer tests. The fill was compacted in oedometers to form samples of 100 mm diameter and height. In addition, compacted fill samples of 38 mm diameter and 89 mm high were tested in a triaxial cell under isotropic compression in the undrained condition. The triaxial tests were performed to measure the pore water pressure generated in samples with different moisture contents when compacted.

With the measured soil compressibility parameters, it is possible to compute the pore water generated using the present method, without additional parameters. The computed pore water pressures are to be compared to the measured values from the triaxial tests.

From the oedometer tests by Penman,<sup>35</sup> sets of Modified Cam-clay parameters were back-figured and are summarised in Table I, where  $\lambda$ ,  $\kappa$ ,  $\Gamma$  and  $M$  are Modified Cam-clay parameters.  $p'_0$  is the maximum isotropic preconsolidation pressure. The gradient of the critical state line  $M$  was assumed to be 1.42 ( $\phi' = 35.0^\circ$ ).

Table I. Modified Cam-clay parameters from oedometer tests by Penman<sup>35</sup>

Initial moisture content $m$ (%)	Initial air content $A$ (%)	$\lambda$	$\kappa$	$\Gamma$	$M^a$	$v'^a$	$p'_0$ (kPa)	Initial porosity	Initial degree of saturation
13.6	0	0.0302	0.00152	1.48	1.42	0.3	10	0.301	1.00
11.2	4.7	0.0182	0.00145	1.41	1.42	0.3	40	0.267	0.823
8.6	9.9	0.00847	0.000981	1.39	1.42	0.3	100	0.263	0.624

<sup>a</sup>Assumed value

Table II. Interpolated modified cam-clay parameters

Initial moisture content $m$ (%)	Initial air content $A$ (%)	$\lambda$	$\kappa$	$\Gamma$	$M^a$	$v'^a$	$p'_0$ (kPa)	Initial porosity	Initial degree of saturation
11.2	3.9	0.0200	0.00147	1.42	1.42	0.3	33	0.269	0.854
9.2	9.8	0.00850	0.00102	1.39	1.42	0.3	96	0.264	0.628

<sup>a</sup>Assumed value

It can be shown that the initial moisture content and therefore the initial degree of saturation of the fills has a significant effect on the virgin compressibility which is governed by parameter  $\lambda$ . An expression for  $\lambda$  as a function of degree of saturation was proposed by Toll,<sup>5</sup> based on laboratory work. Since the moisture contents used in the oedometer and triaxial tests were not identical, it was necessary to determine the parameters corresponding to the triaxial test conditions so that the parameters could be used by the present numerical method to simulate the triaxial tests. For simplicity, the soil parameters ( $\lambda$ ,  $\kappa$  and  $\Gamma$ ) for the triaxial tests were interpolated from those derived in the oedometers, by expressing the parameters as quadratic functions of the degree of saturation. The interpolated values are shown in Table II.

Using the parameters in Table II and taking them as constants, numerical analyses have been carried out on a single finite element to simulate the isotropic compression of the unsaturated samples in the triaxial tests. The degree of saturation–pore water pressure relationship as defined by equation (15) was employed. Figure 4 shows the single finite element and the boundary conditions.

The pore water pressures obtained from the numerical analyses are plotted against the cell pressures and shown in Figure 5. Two hundred time steps were used in each analysis and the number of iterations required for each time step was less than 5. The measurements of the pore water pressure by Penman<sup>35</sup> are also given in the same plot. It can be seen that the numerical analyses provide pore water pressures which agree reasonably well with the measured values.

Additional analyses have also been carried out to examine the sensitivity of the assumed parameter  $M$  on the pore water pressures generated. Using a value of 1 for  $M$  ( $\phi' = 25.4^\circ$ ), the numerical method yielded pore water pressures less than 10 per cent different from those using  $M = 1.42$ .

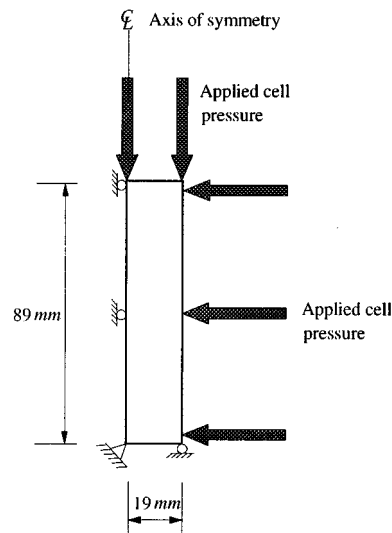
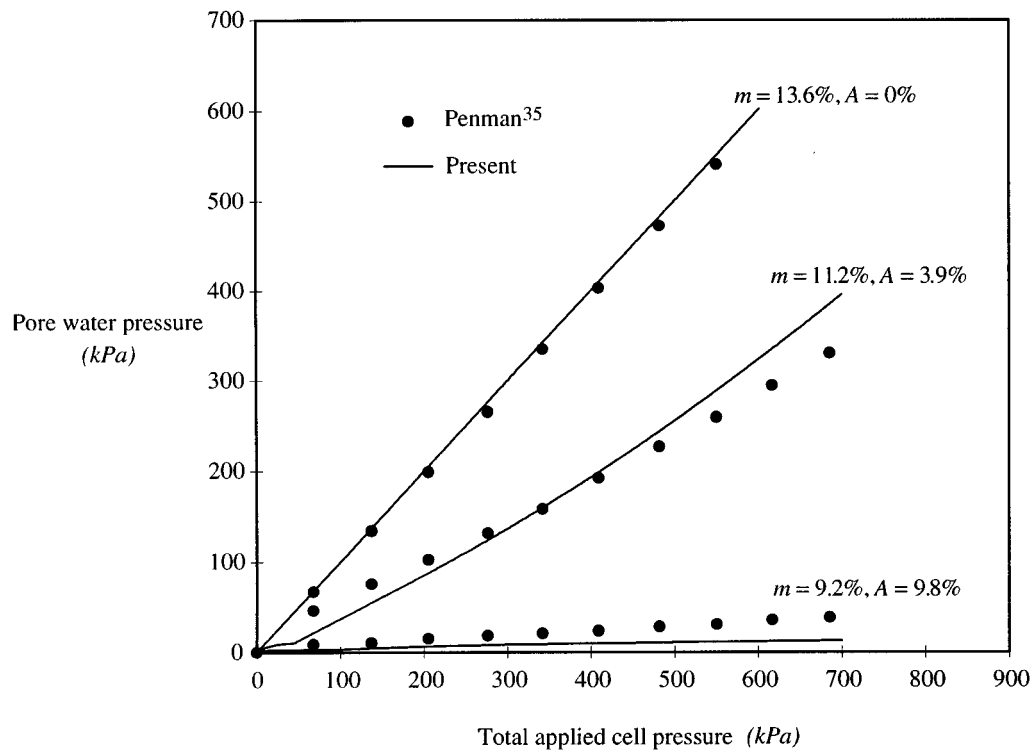


Figure 4. A single element in the triaxial test simulation

Figure 5. Comparison of pore water pressures with direct laboratory measurement by Penman<sup>35</sup>

The numerical results were also compared to those derived using a theoretical approach by Hilf.<sup>36</sup> Hilf's equation can be used to estimate pore water pressures in unsaturated soils for a given volume change. The equation was based on consideration of compressibility of the pore air and solubility of air in water,

$$P = \frac{P_a \Delta}{V_a + hV_w - \Delta} \quad (26)$$

where  $P$  is the total air pressure and is equal to pore pressure if surface tension is neglected.  $P_a$  is the air pressure after initial compaction and can be approximated to atmospheric pressure (101 kPa).  $V_a$  is the volume of free air in the voids after initial compaction, in percentage of initial volume of soil mass, i.e. the air content.  $V_w$  is the volume of water in the voids after initial compaction, in percentage of initial volume of soil mass.  $h$  is Henry's constant of solubility of air in water by volume (0.0198 at 68°F) and  $\Delta$  is the volumetric strain.

However when Hilf's equation is used to calculate  $P$ , the volumetric strain  $\Delta$  must be known. Thus in this example, when using Hilf's equation, the pore water pressures were calculated using the volumetric strains obtained from the numerical analyses. The comparison of the pore water pressures obtained by using the present numerical method and Hilf's equation is shown in Figure 6. Since when using Hilf's equation, the pore water pressures were calculated using the same volumetric strain, the comparison shown in Figure 6 can only be related to the numerical

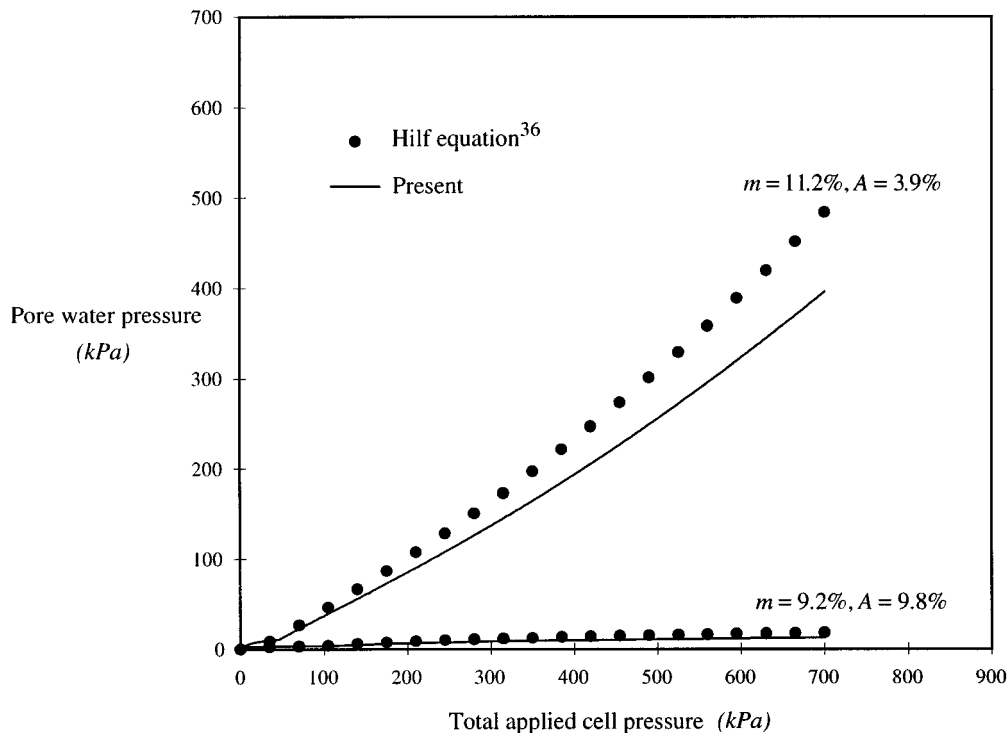


Figure 6. Comparison of pore water pressures with theoretical values calculated using Hilf's equation<sup>36</sup>

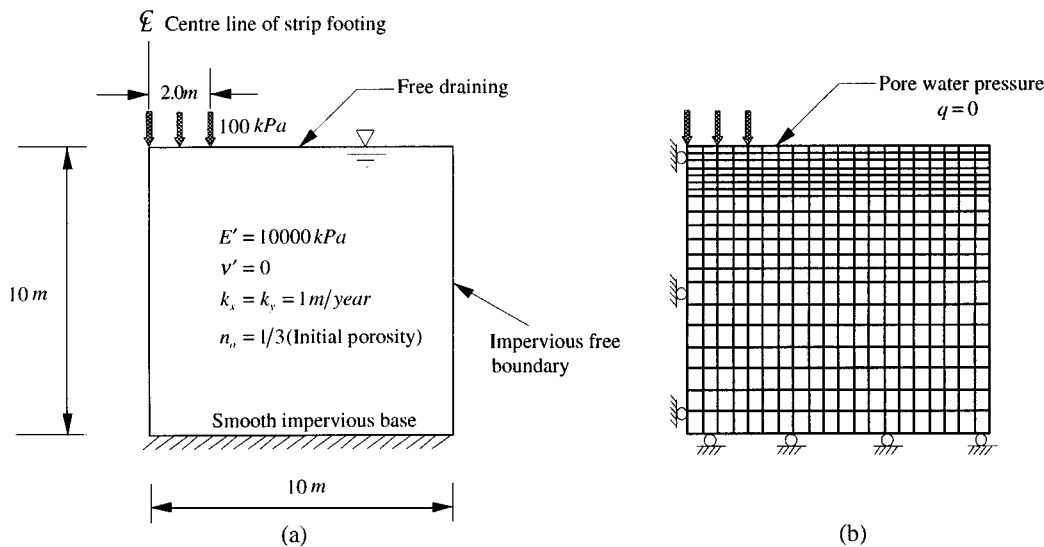


Figure 7. Plane strain consolidation under a strip footing: (a) schematic layout; (b) finite element mesh

solution and bear little relevance to the direct laboratory measurements by Penman.<sup>35</sup> From Figure 6, it can be shown that the pore water pressures calculated using Hilf's equation are in general agreement with the present numerical results.

#### *Plane strain consolidation under a strip footing*

The second example is a classical plane strain problem involving a strip footing. This example allows examination of the numerical method in analysing more complex problems in which the soil can increase or decrease in saturation depending on how the pore water pressure changes at different stages. This example is also useful for studying consolidation behaviour of unsaturated soils with different initial degrees of saturation.

The problem is shown schematically in Figure 7(a) together with the assumed material properties. The footing is completely flexible and the footing pressure is applied instantaneously. For simplicity, the unsaturated soil was assumed to be linear elastic and the same Young's modulus is used for the unsaturated soils with different initial degrees of saturation. The Young's modulus and permeability were assumed to be constant during the analysis.

In total, three analyses were carried out, each with a different degree of saturation at zero pore water pressure  $S_{r0}$  (85, 95 and 100 per cent). The saturated case where  $S_{r0}$  is 100 per cent, was designed to provide a benchmark for the tests. An analytical solution of the Biot's theory for the same strip footing problem on saturated soil was presented by Gibson *et al.*,<sup>37</sup> which is used here for comparison.

A finite element mesh comprising 400 eight-noded quadrilateral elements was employed for this example. The finite element mesh and the boundary conditions can be seen in Figure 7(b). The relationship between degree of saturation and positive pore water pressure as defined by equation (15) was employed. Figure 8 shows the variation of degree of saturation with pore water pressure for different  $S_{r0}$ .

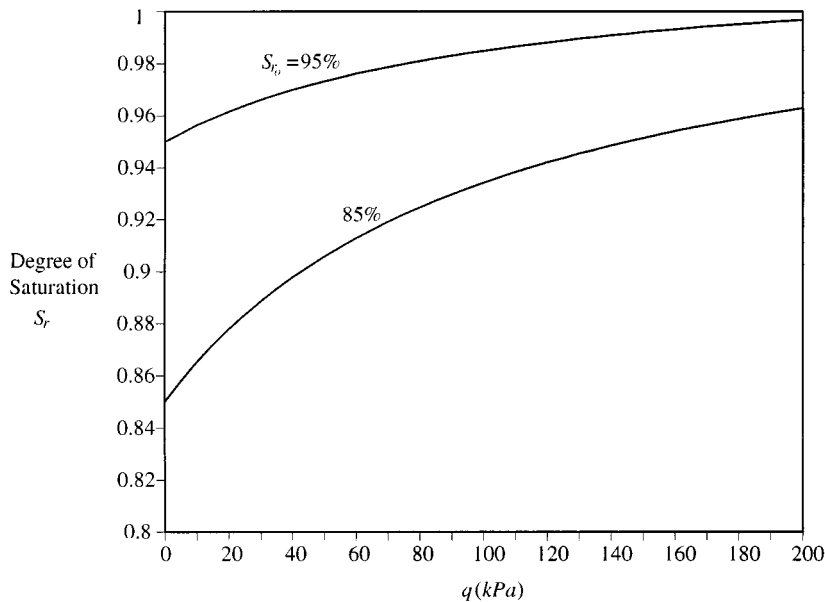


Figure 8. Variation of the degree of saturation  $S_r$  with pore water pressure  $q$

The soil is assumed to be fully immersed initially and the pore water pressure is equal to the geostatic pressure. The  $S_{r_0}$  and the initial pore water pressure were used to define the initial degrees of saturation within the soil mass. It is also assumed that the initial degree of saturation would vary with the geostatic pressure according to the same degree of saturation-pore water pressure relationship (Figure 8). Thus the initial value of  $S_r$  will increase gradually with depth and the initial degree of saturation  $S_r$  at the ground surface will be equal to  $S_{r_0}$  where the pore water pressure is zero.

All the analyses were carried out with 60 time steps and the number of iterations required for each step was less than 5.

In presenting the results, it is convenient to use the dimensionless time factor  $\tau$ ,<sup>37</sup>

$$\tau = \frac{\bar{c}t}{b^2} \quad (27)$$

$$\bar{c} = \frac{2Gk}{\gamma_w} \quad (28)$$

where  $G$  is the elastic shear modulus of the soil skeleton, which is equal to  $E'/2$  when  $\nu' = 0$ .  $k$  denotes the coefficient of permeability and  $\gamma_w$  is unit weight of water, and the footing half width is  $b$ .

From the analyses, the settlements at the mid-point of the footing are obtained and plotted against the logarithm of the time factor  $\tau$  as shown in Figure 9. It can be shown that the immediate settlements occurring in the unsaturated soils were considerably higher than that in

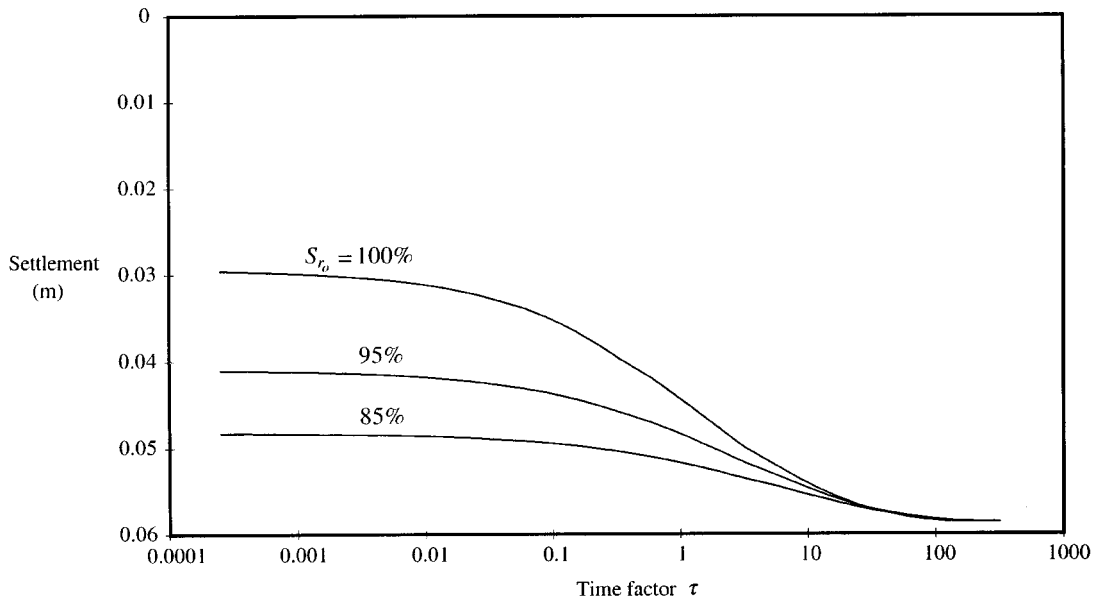


Figure 9. Variation of settlements at the mid-point of the footing with logarithm of time factor

the saturated soil. This is to be expected as unsaturated soils can reduce in volume by compressing the air voids, as compared to saturation soils, where the volume can only be reduced by driving the pore water gradually out of the soil. Since the soil skeleton is treated as an elastic medium, the ultimate settlement is stress path independent and all three cases indicate the same ultimate settlement when all the excess pore water pressures have dissipated.

To investigate the effect to the rate of consolidation when the soil is unsaturated, the definition for degree of consolidation  $U$  proposed by Gibson *et al.*<sup>37</sup> is used.

$$U = \frac{w_t - w_i}{w_{ult} - w_i} \quad (29)$$

where  $w$  is the settlement and subscripts  $t$ ,  $i$  and  $ult$  denote the current, immediate and ultimate settlements.

Figure 10 shows the degree of consolidation computed for the mid-point of the footing for the saturated case, and the analytical solution for the same problem by Gibson *et al.*<sup>37</sup> Good agreement between the two solutions was found.

The degree of consolidation is also plotted for the unsaturated cases as shown in Figure 11. From the figure, it may be seen that the initial degree of saturation of the soil has an appreciable effect on the rate of consolidation and in general the rate of consolidation reduces with the initial degree of saturation. It should be pointed out that the higher immediate settlement obtained when the soil is unsaturated (Figure 9), does not contribute to a higher rate of consolidation according to the current definition of degree of consolidation (equation (29)). In addition, unlike saturated soils, the volume of water expelled from unsaturated soils during consolidation is not necessary equal to the overall volume change of the soil. In this case, the degree of saturation of

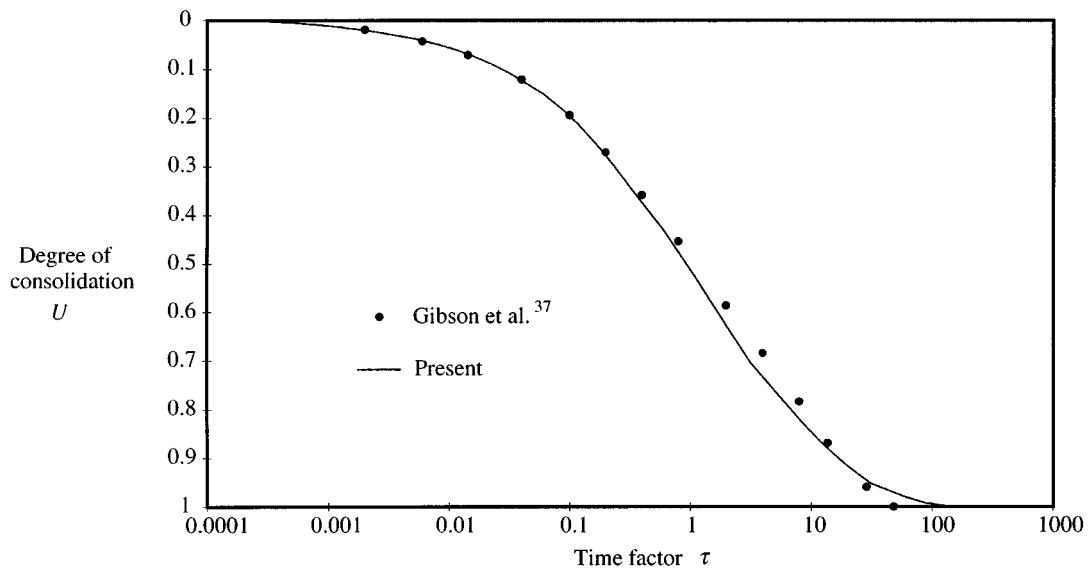


Figure 10. Variation of degree of consolidation with time factor for saturated case

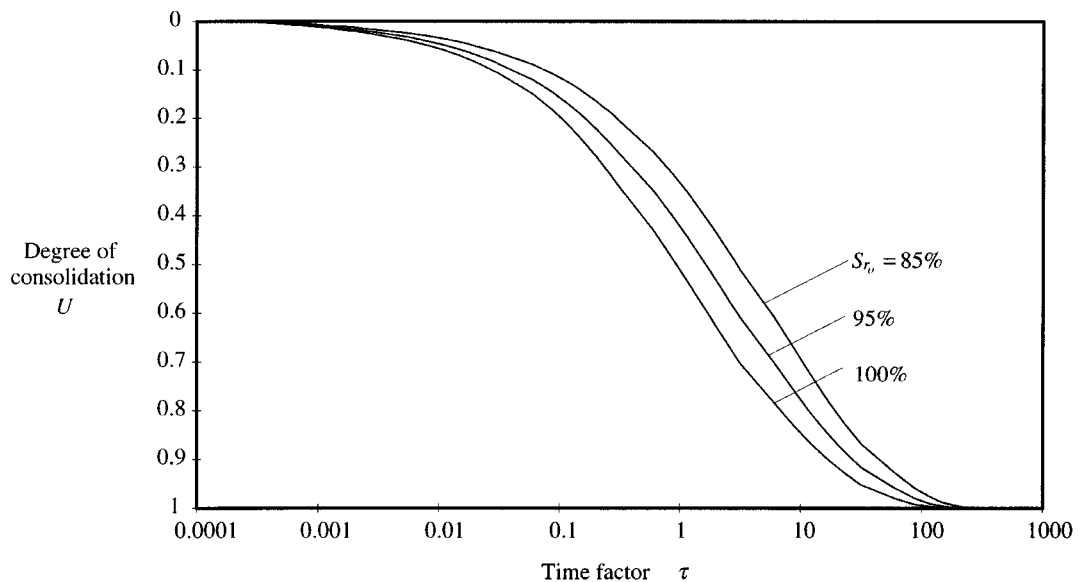


Figure 11. Variation of degree of consolidation with time factor for soils with different initial degrees of saturation

the unsaturated soils would reduce as the pore water pressure drops during consolidation, thus releasing pore water. The amount of water released is in addition to the water expelled due to volume change alone, and the additional amount of water to be drained prolongs the consolidation process.



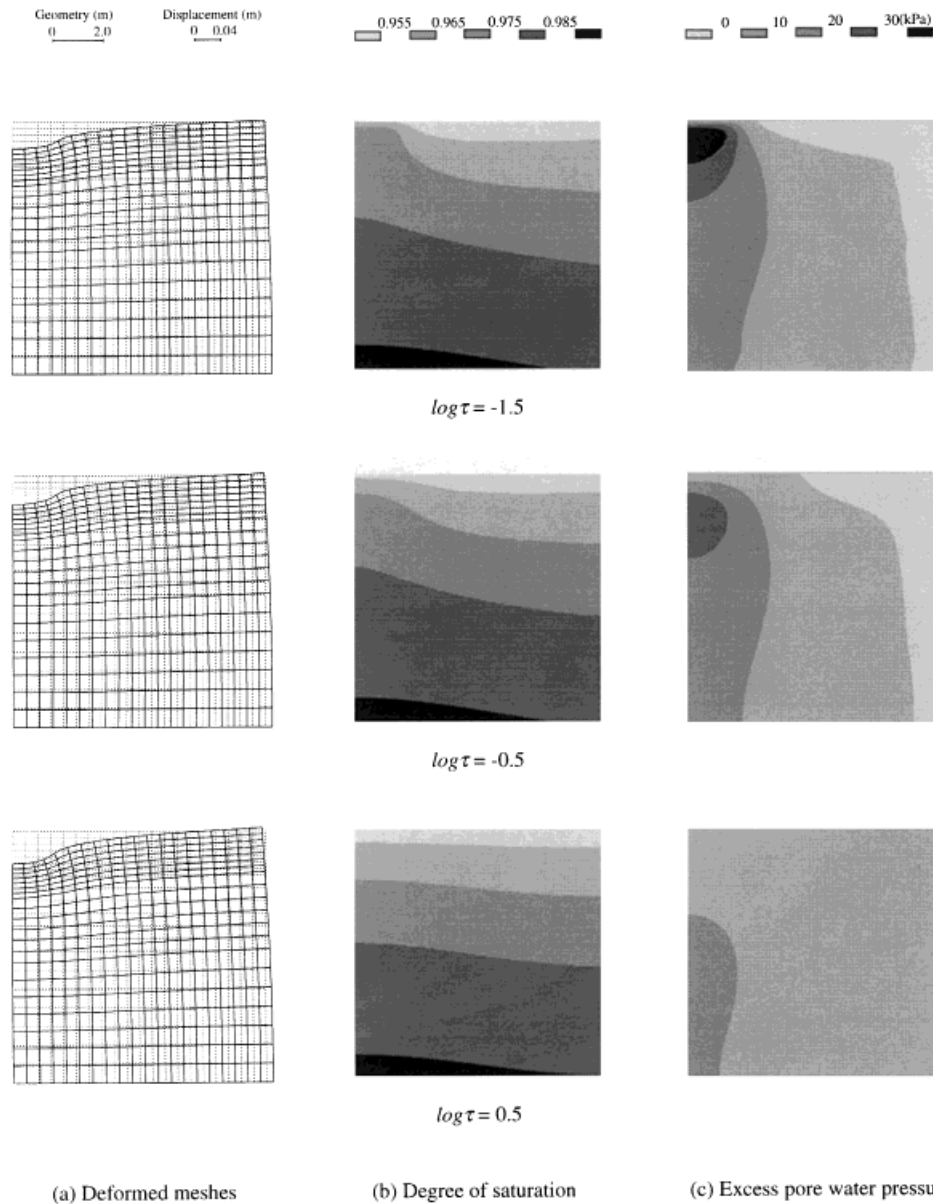


Figure 12. Unsaturated soil ( $S_{r_0} = 95$  per cent) at different time factors: (a) deformed meshes; (b) degree of saturation; (c) excess pore water pressure

To depict the changes in deformation, degree of saturation and excess pore water pressure during consolidation, the deformed meshes and the contours of degree of saturation and excess pore water pressure at different time factors  $\tau$  are plotted in Figure 12. The excess pore water pressures here are the differences between the current and initial pore water pressures.

### Square dam under rapid drawdown

The final example is a classical transient seepage problem of a square dam under rapid drawdown. The problem is shown schematically in Figure 13(a). Different methods for solving the transient problem were found in the literature. Notably, Herbert<sup>38</sup> analysed the problem by adopting a resistance network technique. Bathe *et al.*<sup>39</sup> on the other hand used a finite element method to analyse the same problem by considering flow of water across the transient water table. It is intended to demonstrate that the proposed coupled formulation can be used to analyse the same problem in which the soil is envisaged to de-saturate.

Initially, the water levels on both sides of the dam are equal and flush with the top surface of the dam, and the soil is assumed to be saturated. The water level on the left-hand side of the dam was set to drop instantaneously to the base at  $t = 0$ . Following the external drawdown, the soil mass is expected to release its pore water as the internal water table drops, or from another view point, the soil de-saturates as the internal water table drops.

Since the present formulation is proposed for soils at high degrees of saturation, the formulation will not yield correct deformation when the degree of saturation drops due to lowering of the water table. Therefore, the medium in this example is assumed to be perfectly rigid as those assumed by Herbert<sup>38</sup> and Bathe *et al.*<sup>39</sup> The soil in the present analysis is assumed to be elastic and to have a relatively large Young's modulus in order to limit the deformation. Young's modulus and other material properties are also shown in Figure 13(a).

The permeability of the soil is assumed to drop to 1000th of the original value at  $-1$  kPa. This assumption also implies that there is effectively no water flow in the region above the transient water table.

According to Herbert,<sup>38</sup> the distance that the water table drops at a particular time from the initial position can be related to a parameter  $(k\Delta t)/S_y$ .  $k$  is the permeability below the water table and  $\Delta t$  is the time.  $S_y$  is the specific yield of the soil and was assumed to be constant in Herbert's works. The specific yield  $S_y$  represents the volume of pore water released per unit volume of soil as

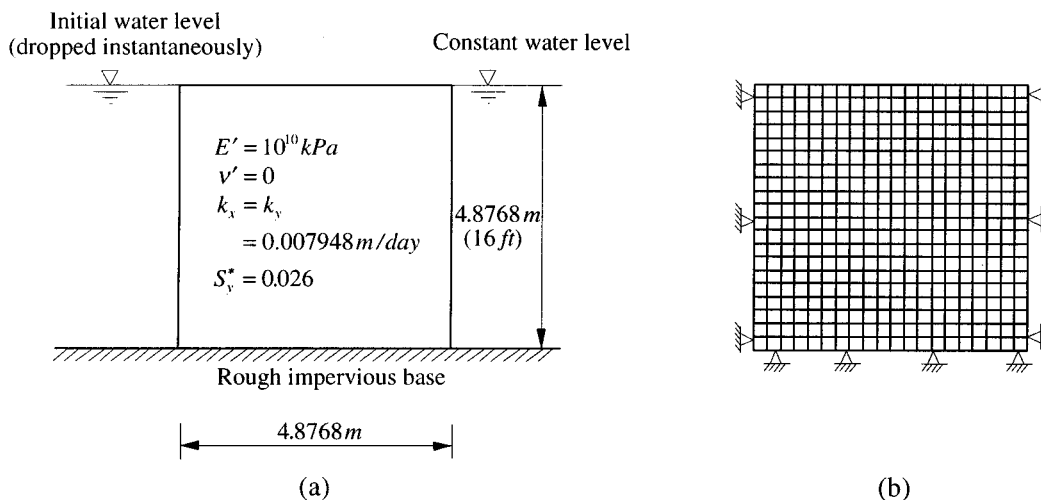


Figure 13. Square dam under rapid drawdown: (a) schematic layout; (b) finite element mesh

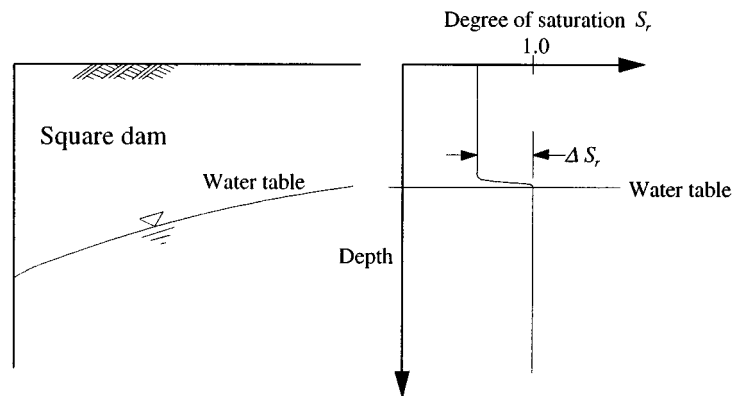
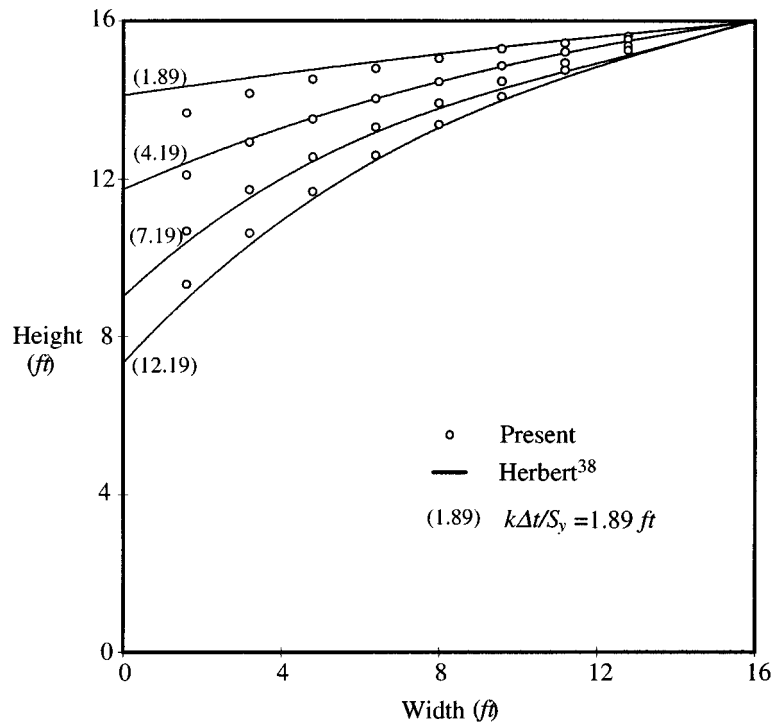


Figure 14. Change of degree of saturation above the water table in square dam

Figure 15. Comparison of water tables obtained at different  $(k\Delta t)/S_y$ 

the water table drops. In the proposed formulation, if a constant specific yield is assumed, a simplified degree of saturation-pore water pressure relationship can be used to simulate a constant  $S_y$ . Figure 14 shows a simplified relationship in which, the degree of saturation for positive pore water pressure is assumed to be 1 and constant. In the negative range of pore water pressure, the degree of saturation reduces sharply (within 1 kPa) to an arbitrary value and remains constant thereafter.



Figure 16. Pore water pressures in square dam under rapid drawdown at  $(k\Delta t)/S_y = 12.19$

This relationship gives an emulated specific yield  $S_y^*$  for the region above the water table, which can be calculated as

$$S_y^* = n\Delta S_r \quad (30)$$

where  $n$  and  $S_r$  are porosity and degree of saturation, respectively. In this example,  $n$  and  $\Delta S_r$  are chosen to be 0.63 and 0.042, respectively.

Figure 13(b) shows the finite element mesh used in the present analysis. The mesh consists of 400 eight-noded quadrilateral elements. It was anticipated that the extent of the seepage face on the left-hand side would change as the water table dropped, the boundary conditions applied on that side were therefore adjusted through iteration in each time step. In total, 50 time steps were used in the analysis and the number of iterations required for each time step was less than 6.

The water tables obtained from the present analysis for different  $(k\Delta t)/S_y$  values are plotted in Figure 15. The solutions by Herbert<sup>38</sup> are also plotted in the same figure for comparison. Despite the fundamental differences in the two methods, the present results are found to be in reasonable agreement with the published results.<sup>38</sup>

For illustration, Figure 16 shows the pore water pressures obtained at  $(k\Delta t)/S_y$  equal to 12.19.

## CONCLUSIONS

A coupled formulation based on a variation of Biot's theory<sup>18</sup> has been developed for unsaturated soils at high degrees of saturation and presented in this paper.

The formulation was solved using the finite element method and was applied to different geotechnical problems as illustration. The encouraging results of these analyses demonstrate that the present method is a useful and flexible tool for analysing these problems which otherwise might have to be analysed with different and specialized methods.

The coupled finite element equations developed are non-linear in nature and iterations were required for solving the equations. The iteration procedure based on Newton–Raphson method had no particular convergence problems and the number of iterations required for each time step was less than 6 for the examples in this paper.

## REFERENCES

1. A. W. Skempton, 'The pore-pressure coefficients A and B', *Géotechnique*, **4**, 143–147 (1954).
2. A. W. Bishop and G. E. Blight, 'Some aspects of effective stress in saturated and partially saturated soils', *Géotechnique*, **13**, 177–197 (1963).
3. D. G. Fredlund and N. R. Morgenstern, 'Stress state variables for unsaturated soils', *J. Geotech. Engng. Div. ASCE*, **103**(GT5), 447–466 (1977).
4. E. E. Alonso, A. Gens and A. Josa, 'A constitutive model for partially saturated soils', *Géotechnique*, **40**, 405–430 (1990).
5. D. G. Toll, 'A framework for unsaturated soil behaviour', *Géotechnique*, **40**, 31–44 (1990).
6. S. J. Wheeler, 'An alternative framework for unsaturated soil behaviour', *Géotechnique*, technical note, **41**, 257–261 (1991).
7. D. G. Fredlund and H. Rahardjo, 'An overview of unsaturated soil behaviour', *Unsaturated Soils, Geotechnical Special Publication No. 39*, ASCE, 1993, pp. 1–31.
8. S. Bonelli and D. Poulain, 'Unsaturated elasto-plastic model applied to homogeneous earthdam behaviour', in E. E. Alonso and P. Delage (Eds), *Unsaturated Soils/Sols Non Saturés*, 1995, pp. 265–271.
9. J. Ghaboussi and E. L. Wilson, 'Flow of compressible fluid in porous elastic media', *Int. J. Numer. Meth. Engng.*, **5**, 419–442 (1973).
10. K. Akai, Y. Ohnishi, T. Murakami and M. Horita, 'Coupled stress flow analysis in saturated-unsaturated medium by finite element method', in W. Wittke, (Ed.) *Proc. 3rd Int. Conf. Numer. Meth. Geomech.*, Aachen, vol. 1, 1979, pp. 241–250.
11. C. S. Chang and J. M. Duncan, 'Consolidation analysis for partly saturated clay by using an elastic-plastic effective stress-strain model', *Int. J. Numer. Anal. Meth. Geomech.*, **7**, 39–55 (1983).
12. L. Lam, D. G. Fredlund and S. L. Barbour, 'Transient seepage model for saturated-unsaturated soil systems: a geotechnical engineering approach', *Can. Geotech. J.*, **24**, 565–580 (1987).
13. Y. Kohgo and T. Yamashita, 'Finite element analysis of fill type dams-stability during construction by using the effective stress concept', in G. Swoboda (Ed.), in *Proc. 6th Int. Conf. Numer. Meth. Geomech.*, Innsbruck, vol. 2, 1988, pp. 1315–1322.
14. H. R. Thomas and S. W. Rees, 'Modeling field infiltration into unsaturated clay', *J. Geotech. Engng. Div.*, ASCE, **116**(10), 1483–1501 (1990).
15. E. E. Alonso, F. Battle, A. Gens and A. Lloret, 'Consolidation analysis of partially saturated soils—Application to earthdam construction', *Proc. 6th Int. Conf. on Numer. Meth. in Geomech.*, Innsbruck, vol. 2, 1988, pp. 1303–1308.
16. N. Khalili and M. H. Khabbaz, 'On the theory of three-dimensional consolidation in unsaturated soils', in E. E. Alonso and P. Delage, (Eds), *Unsaturated Soils/Sols Non Saturés*, 1995, pp. 745–750.
17. D. Gawin, L. Simoni and B. A. Schrefler, 'Numerical model for hydro-mechanical behaviour in deformable porous media: a benchmark problem', *Proc. 9th Int. Conf. on Computer Methods and Advances in Geomechanics*, Wuhan, vol. 2, 1997, pp. 1143–1148.
18. M. A. Biot, 'General theory of three-dimensional consolidation', *J. Appl. Phys.*, **12**, 155–164 (1941).
19. R. S. Sandhu and E. L. Wilson, 'Finite-element analysis of seepage in elastic media', *J. Eng. Mech. Div.*, ASCE, **95**(EM3), 641–652 (1969).
20. J. C. Small, K. L. A. Ng and J. P. Hsi, 'Excavation and construction problems involving porous media', A. P. S. Selvadurai (Ed.), *Mechanics of Poroelastic Media*, Kluwer Academic Publishers, Netherlands, 1996, pp. 181–195.
21. H. J. Siriwardane and C. S. Desai, 'Two numerical schemes for nonlinear consolidation', *Int. J. Numer. Meth. in Eng.*, **17**(3), 405–426 (1981).
22. A. W. Bishop and D. J. Henkel, *The Measurement of Soil Properties in the Triaxial Test*, 2nd ed, Edward Arnold, London, Appendix 6, 1962.
23. H. Bouwer, 'Unsaturated flow in ground-water hydraulics', *J. Hydraulics Div.*, ASCE, **90**(HY5), 121–144 (1964).
24. C. S. Desai and W. C. Sherman, 'Unconfined transient seepage in sloping bands', *J. Soil Mech. Found. Div.*, ASCE, **97**(2), 357–373 (1971).
25. D. N. Cathie and R. Dungar, 'The influence of the pressure-permeability relationship on the stability of a rock-filled dam', in D. J. Naylor, K. G. Stagg and O. C. Zienkiewicz, Swansea (Eds.), *Criteria and Assumptions for Numerical Analysis of Dams*, 1975, pp. 830–845.
26. K. J. Bathe and M. R. Khoshgoftaar, 'Finite element free surface seepage analysis without mesh iteration', *Int. J. Numer. Anal. Meth. Geomech.*, **3**, 13–22 (1979).
27. E. Rank and H. Werner, 'An adaptive finite element approach for the free surface seepage problem', *Int. J. Numer. Meth. Engng.*, **23**, 1217–1228 (1986).
28. S. P. Neuman, 'Saturated-unsaturated seepage by finite elements', *J. Hydraulics Div.*, ASCE, **99**(HY12), 2233–2250 (1973).
29. A. Lloret and E. E. Alonso, 'State surfaces for partially saturated soils', *Proc. 11th Int. Conf. Soil Mech. Found. Engng.*, **2**, 557–562 (1985).
30. J. Lowe and T. C. Johnson, 'Use of back pressure to increase the degree of saturation of triaxial test specimens', *Proc. ASCE Research Conf. on the Shear Strength of Cohesive Soils*, Boulder, Colo., 1960.

31. J. K. Mitchell, D. R. Hooper and R. G. Campanella, 'Permeability of compacted clay', *J. Soil Mech. Found. Div.*, ASCE, **91**(SM4), 41–65 (1965).
32. J. C. Small, J. R. Booker and E. H. Davies, 'Elasto-plastic consolidation of soil', *Int. J. Solids Struct.*, **12**, 431–448 (1976).
33. C. S. Desai, 'Finite element residual schemes for unconfined flows', *Int. J. Numer. Meth. in Engng.*, **10**, 1415–1418 (1976).
34. G. C. Li and C. S. Desai, 'Stress and seepage analysis of earth dams', *J. Geotech. Engng. Div.*, ASCE **109**(GT7), 946–960 (1983).
35. A. D. M. Penman, 'Construction pore pressures in two earth dams', *Clay Fills*, ICE, 177–187 (1978).
36. J. W. Hilf, 'Estimating construction pore pressures in rolled earth dams', *Proc. 2nd Int. Conf. Soil Mech. Found. Engng.*, **3**, 234–240 (1948).
37. R. E. Gibson, R. L. Schiffman and S. L. Pu, 'Plane strain and axially symmetric consolidation of a clay layer on a smooth impervious base', *Quart. J. Mech. Appl. Math.*, **23**(4), 505–520 (1970).
38. R. Herbert, 'Time variant ground water flow by resistance network analogues', *J. Hydrol.*, **6**, 237–264 (1968).
39. K. J. Bathe, V. Sonnad and P. Domigan, 'Some experiences using finite element methods for fluid flow problems', *Proc. 4th Int. Conf. Finite Element Methods in Water Resources*, Hannover, 1982, pp. 9.3–9.16.